frontiers | Frontiers in Ecology and Evolution

TYPE Brief Research Report
PUBLISHED 05 December 2023
DOI 10.3389/fevo.2023.1288596

OPEN ACCESS

EDITED BY
Miao Lv,
Southwest Jiaotong University, China

REVIEWED BY
Risheng Xu,
Northwestern Polytechnical University, China
Dannise V. Ruiz-Ramos,
University of Maryland Eastern Shore, United States
Ronen Liberman,
Tel Aviv University, Israel

*CORRESPONDENCE
Colin J. Anthony
colin_anthonynw@outlook.com

RECEIVED 04 September 2023
ACCEPTED 21 November 2023
PUBLISHED 05 December 2023

CITATION
Anthony CJ, Lock C, Taylor BM and Bentlage B (2023) Cellular plasticity facilitates phenotypic change in a dominant coral's Symbiodiniaceae assemblage. *Front. Ecol. Evol.* 11:1288596. doi: 10.3389/fevo.2023.1288596

Cellular plasticity facilitates phenotypic change in a dominant coral's Symbiodiniaceae assemblage

Colin J. Anthony*, Colin Lock, Brett M. Taylor and Bastian Bentlage

Marine Laboratory, University of Guam, Mangilao, GU, United States

Coral-associated dinoflagellates (Symbiodiniaceae) are photosynthetic endosymbionts that influence coral acclimation, as indicated by photo-endosymbiotic phenotypic variance across different environmental conditions. Symbiont shuffling (shifts in endosymbiont community composition), changes in endosymbiont cell density, and cellular plasticity have all been proposed as acclimation mechanisms. However, few studies have been able to partition which of the three strategies were responsible for observed phenotypic variance. Using a combination of metabarcoding and flow cytometry, we simultaneously characterized *Acropora pulchra*-associated Symbiodiniaceae assemblages at the community, population, and individual level under natural environmental conditions to deduce whether seasonal phenotypic change and site-related phenotypic variation of Symbiodiniaceae assemblages is a product of symbiont shuffling or cellular plasticity. Symbiodiniaceae assemblages displayed season-specific phenotypic variance, while Symbiodiniaceae community composition was geographically structured and cell density showed limited data structure. Based on these patterns, we reveal that cellular plasticity of Symbiodiniaceae was the source of a phenotypic variation, thus indicating that cellular plasticity is a mechanism for acclimation to mild environmental change.

KEYWORDS

phenotype, plasticity, acclimation, coral reefs, Symbiodiniaceae, *Acropora*

1 Introduction

Symbiodiniaceae are dinoflagellates known for their endosymbiotic relationship with many marine invertebrates including Cnidaria, Mollusca, Porifera, Platyhelminthes, Foraminifera, and Ciliata (LaJeunesse et al., 2018). The ecological success of reef-building corals has been attributed to this endosymbiotic relationship with Symbiodiniaceae (Gault et al., 2021). Corals are highly dependent on Symbiodiniaceae for nutrient acquisition and effective calcification (Falkowski et al., 1984; Muscatine et al., 1984; Ezzat et al., 2017; Matthews et al., 2017), but environmental stress can cause a

breakdown of this photo-endosymbiotic relationship, leading to the expulsion of Symbiodiniaceae from the host (coral bleaching) and often death (Brown, 1997). Climate change has increased the frequency and severity of coral bleaching globally (Hughes et al., 2017) and the survival of corals has been linked to differences in the ecological tolerances of Symbiodiniaceae (Thornhill et al., 2014; Parkinson et al., 2015; Howe-Kerr et al., 2020).

Acropora pulchra (Brook, 1891) is a fast-growing staghorn coral, providing substantial reef structure and habitat for a diverse assemblage of fish and invertebrates. In Guam, *A. pulchra* is the most abundant staghorn coral, dominating shallow reef flats. However, *A. pulchra* is highly susceptible to elevated sea surface temperatures, exposure to extreme low tides, and disease (Raymundo et al., 2017). In Guam, two consecutive years of anomalously high sea surface temperatures combined with extreme tides caused a decline of ~33% of *A. pulchra*'s distribution (Raymundo et al., 2017; Raymundo et al., 2019). Stress events and extreme environments naturally select for resilient genotypes (Fine et al., 2013; Roche et al., 2018; Leiva et al., 2023), yet *A. pulchra* populations around Guam are highly clonal (Rios, 2020). In highly clonal populations, coral genotype has been found to be a minor determinant of selection, suggesting that Symbiodiniaceae are key determinants of coral survival in such populations (Swain et al., 2020). As such, we expect Guam's remaining *A. pulchra* populations to be dominated by resilient Symbiodiniaceae assemblages. The characterization of Guam's dominant reef flat staghorn corals, which have survived several recent coral bleaching and stress events may provide succinct and novel insight on the response of Symbiodiniaceae to environmental change and their role in coral survival.

In the short term (within a generation), Symbiodiniaceae communities seem largely controlled by the host, while in the long term (across generations), environmental change may shift symbiont community composition (Baker et al., 2018; Camp et al., 2019; Howe-Kerr et al., 2020). If environments change, successful acclimation of corals may be caused by shifts in endosymbiont community composition, known as symbiont shuffling (Buddemeier and Fautin, 1993; Baker, 2003; Jones et al., 2008). For example, *Durusdinium* is more common than other Symbiodiniaceae genera in stressful environments (Fabricius et al., 2004; LaJeunesse et al., 2010) or after acute stress events (Baker et al., 2004; Berkelmans and van Oppen, 2006). However, endosymbiotic Symbiodiniaceae community composition can also be remarkably stable (Rouzé et al., 2019), indicating a high level of host-symbiont specificity, thus requiring a high acclimation potential through phenotypic plasticity to survive environmental change (Goulet, 2006). Species of Symbiodiniaceae have been experimentally shown to have varying rates of plasticity in response to environmental change (Mansour et al., 2018), which could lead to a change in Symbiodiniaceae assemblage composition or abundance. Therefore, the acclimation strategy of a coral-associated Symbiodiniaceae assemblage may be facilitated by either symbiont shuffling, cell density regulation, or cellular plasticity and is dependent on its constituent members and its environment (Jones and Yellowlees, 1997; Baker, 2003; Baker et al., 2004; Goulet, 2006).

Phenotypic variance within and across Symbiodiniaceae assemblages may be caused by the presence of diverse symbiont clades that display different phenotypes. However, in low complexity Symbiodiniaceae assemblages, dominated by a single symbiont clade, variations in observed phenotypes may be interpreted as the result of cellular plasticity (Anthony et al., 2023). Symbiodiniaceae individuals have several mechanisms for acclimation through cellular plasticity. Generally, Symbiodiniaceae acclimation revolves around modifying the efficiency and productivity of their photosystem, as it is the most direct way to regulate ATP and NADPH formation, and in turn, the quantity of harmful and beneficial metabolic byproducts (Oakley et al., 2014). Photosystem acclimation is typically tied to the modification of photosystem photochemistry (Warner et al., 1996; Ulstrup et al., 2008; Nitschke et al., 2018). The physical reorganization and regulation of photopigments or adjustments to cell morphology can also mitigate stress and promote successful acclimation to different conditions and may be a better representation of long term (months versus days) system regulation (Johnsen et al., 1994; Sawall et al., 2014; Xiang et al., 2015; Oliveira et al., 2022).

Photoacclimation *in situ* is well studied during seasonal change (Warner et al., 2002; Ulstrup et al., 2008; Sawall et al., 2014) and along light attenuation gradients including depth (Iglesias-Prieto et al., 2004; Frade et al., 2008; Lesser et al., 2010; Cooper et al., 2011) and turbidity (Hennige et al., 2008; Suggett et al., 2012). This research typically attributes observed photoacclimation patterns to (1) changes in community composition, (2) endosymbiotic cell densities, and (3) cellular plasticity. However, research often relies on pulse-amplitude-modulated (PAM) fluorometry (Warner et al., 1996), multi-spectral fluorometry (Hoadley et al., 2023), or high performance liquid chromatography (HPLC) (Mantoura and Llewellyn, 1983) to characterize the state of endosymbiont photosystems. These methods can be standardized to 'phenotype' coral holobionts (Voolstra et al., 2020), but cannot provide insight into phenotypic variance of individual symbiont cells. Alternatively, flow cytometry is an underutilized methodology that can rapidly quantify symbiont cells (Krediet et al., 2015) and generate phenotypic profiles on a per cell basis, thus providing the resolution required to identify the source of phenotypic variation (Apprill et al., 2007; Anthony et al., 2023).

Symbiont shuffling, cell density regulation, and cellular plasticity have all been proposed as mechanisms for Symbiodiniaceae to adjust to environmental change (Jones and Yellowlees, 1997; Baker, 2003; Baker et al., 2004; Goulet, 2006). Despite the plethora of knowledge on Symbiodiniaceae response to their environment, most research has not closed the gap in resolving the relationship between phenotypic variance, shifts of Symbiodiniaceae community composition, and cellular plasticity of the existing community. Here we help narrow this knowledge gap by simultaneously characterizing the *A. pulchra*-associated Symbiodiniaceae assemblage at the community (biodiversity), population (cell density), and individual level (phenotype) under natural environmental conditions. By comparing ITS2 type profiles to flow cytometric phenotypic profiles, we were able to test whether Symbiodiniaceae phenotypic variation was caused by cellular plasticity or symbiont genotype.

2 Materials and methods

2.1 Coral colonies

To identify the dynamics of Symbiodiniaceae assemblages under natural seasonal fluctuation on an island-wide scale, four plots of *A. pulchra* from five reef flats (20 plots total) were GPS-tagged around the island of Guam: Urunao (N 13.63672° E 144.84527°), West Agaña (N 13.47993° E 144.74278°), Luminao (N 13.46584° E 144.64496°), Cocos Lagoon (N 13.24596° E 144.68475°) and Togcha (N 13.36865° E 144.774967°) (Figures 1A–F). From this point forward sites will be referred to as North (Urunao), Northwest (West Agaña), West (Luminao), South (Cocos Lagoon), and East (Togcha). Colonies within each plot were photographed using an Olympus Tough TG-6.

2.2 Environment

To characterize island-wide seasonal environmental changes, average sea surface temperature (SST) and precipitation data were obtained for Guam in 2021 from the NOAA Coral Reef Watch (Liu et al., 2018; www.coralreefwatch.noaa.gov, accessed 10 February 2022) and the Global Historical Climatology Network (Menne et al., 2012; www.ncdc.noaa.gov/cdo-web/datasets/GHCND/stations/GHCND : GQW00041415/detail; accessed 10 February 2022), respectively. Bleaching risk was assessed using NOAA's 5km regional virtual field station for Guam (Liu et al., 2018; https://coralreefwatch.noaa.gov/product/vs/gauges/guam.php, accessed 10 February 2022). Historical wave height, period, and cardinal direction was provided by the Pacific Islands Ocean Observing System (PacIOOS; www.pacioos.org, accessed 10 February 2022) for 2012-2022 from wave buoys at Ritidian Point (N Guam) and Ipan (SE Guam).

2.3 Tissue sampling

From each site (Figures 1A–F), three tissue samples per plot were collected by cutting two-centimeter-long pieces from at least three centimeters below the axial growth tip. This was repeated for all 20 GPS-tagged plots at two time points within 2021: (1) 30 April – 18 May and (2) 28 July – 15 August. Each sampling effort yielded 12 tissue samples per site and 60 tissue samples per time point. If more than one colony existed near the GPS-tagged plot (North and East), photographs were referenced on-site to ensure that the same colonies were repeatedly sampled within each plot. All samples were immediately flash-frozen in liquid nitrogen on site, then stored at -80°C until processing. These samples were subsequently used to quantify Symbiodiniaceae community composition, cell density, and phenotypic variation, deriving all variables from the same source fragment.

2.4 Symbiodiniaceae cell density

Coral tissue (120 samples) was airbrushed from the skeleton with filtered seawater (FSW) and homogenized using a vortexer followed by syringe needle-shearing, and then processed using the protocol described in Anthony et al. (2023).

Absolute cell counts were obtained by multiplying flow cytometry-generated cell concentrations with each sample's dilution factor and tissue homogenate volume to determine total cell count for each coral tissue fragment. Cell density per cm^2 (Equation 1) was obtained by the normalization of flow cytometry-derived cell counts to the source fragment's skeletal surface area. To determine skeletal surface area, a three-dimensional model was created for each coral fragment built from point clouds with 0.010 mm point spacing generated by a jewelry scanner (D3D-s, Vyshneve, Ukraine). Prior to scanning, coral fragments were coated with SKD-S2 Aerosol (Magnaflux, Glenview, IL) to reduce skeletal light refraction. Point clouds of each fragment were imported into MeshLab v2020.04 (Cignoni et al., n.d.) to generate a surface mesh by Poisson surface reconstruction. Portions of the fragment that were not covered in tissue prior to airbrushing were removed from the reconstructed surface prior to surface area estimation.

$$CellDensity = \frac{(CellCount)(Dilution)(TotalHomogenateVolume)}{SampleSurfaceArea}$$

2.5 Symbiodiniaceae phenotyping

As described by Anthony et al. (2023), three flow cytometric signatures (red fluorescence, forward scatter, and side scatter) were used to generate a phenotypic profile for Symbiodiniaceae cells from each of the 120 tissue samples. Red fluorescence represents relative photopigment abundance (Lesser, 1996; Lee et al., 2012; Cooper et al., 2014). Side scatter is a representation of cell shape or roughness, and forward scatter is a representation of cell size or cell volume (Mullaney et al., 1969; Steen, 1980; Shapiro, 2003; Tzur et al., 2011). The full protocol with details on sample preparation, data curation, and analysis is publicly available on protocols.io (dx.doi.org/10.17504/protocols.io.dm6gpjr2jgzp/v3).

2.6 Symbiodiniaceae high-throughput ITS2 metabarcoding

Genomic DNA was extracted from tissue aliquoted prior to airbrushing (see '*Symbiodiniaceae cell density*' above) using a Qiagen DNeasy PowerSoil Pro Kit (Qiagen, Hilden, Germany) on a Qiacube connect liquid handling system. The ITS2 region was amplified *via* PCR with SYM_VAR_5.8S2 and SYM_VAR_REV primers (Hume et al., 2018) using 3 µL of DNA (10 ng/µl), 3 µl of 10 µM primer, 2.4 µl of 2.5 mM dNTP, 18.6 µl water, 3 µl buffer (10x), and 0.15 µl Taq (TaKaRa Taq DNA Polymerase 1U, Takara Bio USA, Ann Arbor, MI). The PCR profile included 26 cycles of 95°C for 40 s, 59°C for 120 s, 72°C for 60 s, and a final extension at 72°C for 420 s. ITS2 amplicons were multiplexed and sequenced on a NovaSeq 6000 (Illumina, San Diego, CA, USA) to generate 250 bp paired-end reads. Of the 120 samples extracted, 92 samples were successfully sequenced. After NovaSeq sequencing (Illumina, San Diego CA), metabarcoding data was preprocessed with

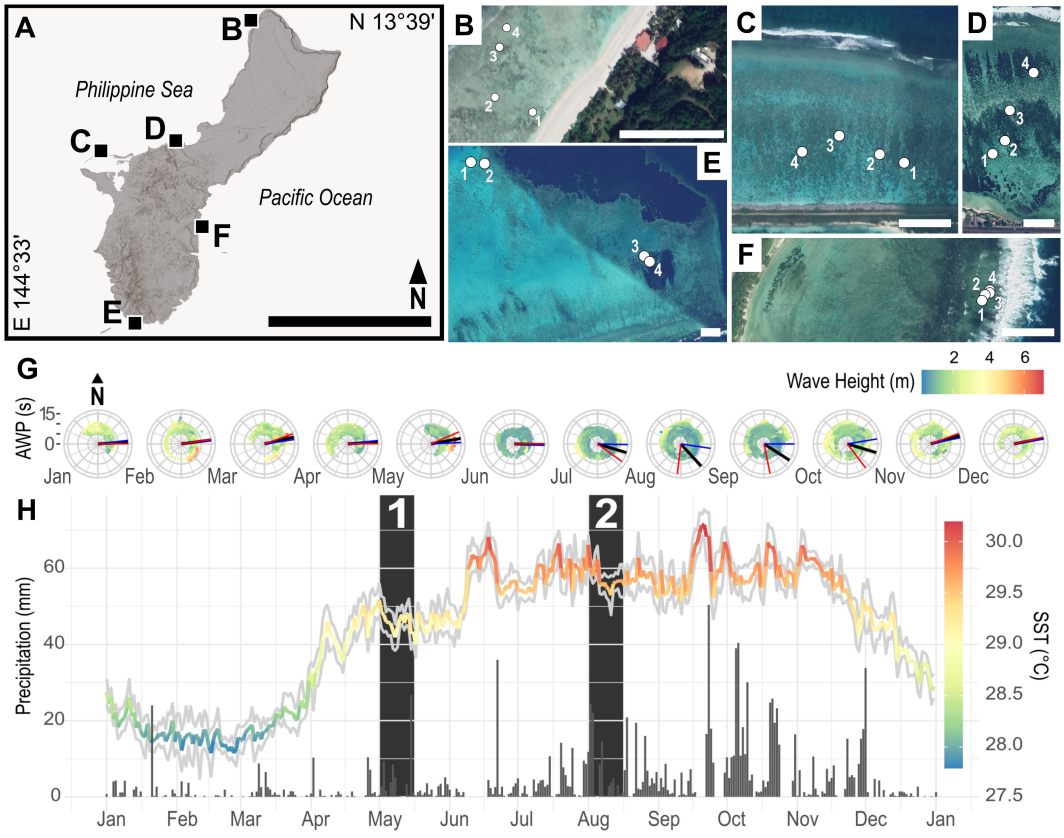

FIGURE 1
(A) Sampling sites in Guam (scale: 20 km) with each square indicating the location of a reef flat sampled for this study: **(B)** Urunao (North), **(C)** West Agaña (Northwest), **(D)** Luminao (West), **(E)** Cocos Lagoon (South), and **(F)** Togcha (East). **(B–F)** Within each site, four plots (1-4) of *A. pulchra* were georeferenced for repeated sampling. Images provided by Google Earth Pro v7.3.4.8248 (scale: 100 m). **(G)** Spectral polar plots of aggregated historical wave data from Ritidian (red lines) and Ipan (blue lines) wave buoys. Monthly mean wave direction (black lines) indicated prevailing swells from the East, the windward side of Guam. (Provided by PacIOOS; www.pacioos.org). **(H)** Average sea surface temperature (SST) (spectral line) and precipitation (grey bars) for 2021 showed distinct seasonal patterns. (Provided by NOAA Coral Reef Watch; www.coralreefwatch.noaa.gov) The first set of samples was collected in the first two weeks of May (1) during the transitional warming period, while the second set of samples was collected in the first two weeks of August (2) during the hot, rainy season.

the SymPortal pipeline (Hume et al., 2019). Raw reads are available through NCBI's GenBank (BioProject PRJNA1043707), while preprocessed ITS2 data can be obtained from www.symportal.org (accession: 20220419_GuamWild_bentlage). Relative ITS2 sequence abundances and type profiles were normalized and visualized as per Eckert et al. (2020). Curated datasets have been deposited within this manuscript's associated GitHub repository (https://github.com/AnthonyCuog/SpatiotemporalPhenotypicProfiling).

2.7 Statistical analysis

Flow cytometric data (cell density, red fluorescence, forward scatter, and side scatter) violated the assumption of parametric tests of a normal data distribution, as determined by Shapiro-Wilk tests ($p < 0.001$); therefore all statistical tests were non-parametric and did not assume normality.

To identify possible correlations between cell density, red fluorescence, side scatter, and forward scatter, non-parametric Spearman correlations were calculated for two groupings of paired dependent variables: (1) cell density, red fluorescence, side scatter, and forward scatter averaged to the fragment-level replicate and (2) red fluorescence, side scatter, and forward scatter without any value summarization (single symbiont cells), given that flow cytometry automatically produces paired data for each cell detected (Anthony et al., 2023). Calculations were completed using rstatix v0.7.1 (Kassambara, 2022).

Repeated measures, univariate analyses of variance (RM-ANOVA) were performed to quantify the factorial contribution of time, site, and plot to the data structure of cell density, red fluorescence, forward scatter, and side scatter using the MANOVA.RM package v0.5.3 (Friedrich et al., 2022). A repeated measures, multivariate analysis of variance (RM-MANOVA) was also completed for grouping of red fluorescence, forward scatter, and side scatter to determine their contribution to the variation of cell phenotypes. For these tests, plot was treated as a fixed effect for the repeated sampling of colonies within each plot and was only analyzed as a nested factor within each site to control the variation of site-specific plot location (Figure 1). Main and interaction effects were resampled with 1000 non-parametric bootstrap replicates and corrected p-values were calculated for type statistics. This

test neither assumes multivariate normality nor covariance matrix specificity, making it robust to repeated measure designs with factorial nesting not requiring any data transformation to adhere to model assumptions (Friedrich et al., 2019). Prior to any statistical tests, 1000 observations for each group were randomly sampled for each cytometry replicate (often from a sample size of > 100,000 per cell measurements) to reduce the computational requirements of statistical tests and decrease the likelihood of effect size and strength overinterpretation.

In addition to the repeated measures tests, data from the 40 sampling events (five sites, two timepoints, and 20 colonies) were evaluated with non-parametric pairwise Dunn's tests, as integrated in the FSA package v0.9.3 (Ogle et al., 2022). Statistical outputs were then converted to statistical groups using _rcompanion v2.4.21 (Mangiafico, 2023). Each sample distribution was assigned to a statistical group (a-s) based on the results of pairwise Dunn's tests, which better visualized data structure and similarity, thus improving the interpretation of previously calculated repeated measures tests. A distribution would be in the same group as another distribution if they were not statistically different (e.g., $p > 0.001$), while distributions would appear in different groups if they were statistically different (e.g., $p < 0.001$). Cell density data distributions were grouped with a standard threshold of $p = 0.05$, while phenotypic measurements were grouped with a threshold of $p = 0.001$ to avoid the overinterpretation of effect sizes made stronger by a high sample size ($n = 1000$) (c.f. Anthony et al., 2023).

Symbiodiniaceae community structure was compared across sites (North, Northwest, West, South, East) and seasons (May, August). Multivariate homogeneity of dispersion (PERMDISP), pairwise permutation tests (PERM), and a permutational multivariate analysis of variance (PERMANOVA) were conducted on normalized ITS2 type profiles as needed using Vegan v2.5-7 (Oksanen et al., 2019) and pairwise Adonis v0.4 (Martinez Arbizu, 2017) packages. PERMDISP and permutation tests used Bray-Curtis dissimilarity. Permutation tests were run with 9999 replicates.

To test whether underlying phenotypic variation was caused by cellular plasticity or ITS2 type-specific phenotypes, the North Site's ITS2 type profiles, identified by metabarcoding, were mapped to their fragment's associated phenotypic profile generated by flow cytometry. Phenotypic measurements for the North (the only site with heterogeneous Symbiodiniaceae biodiversity) were compared using a combination of Kruskal-Wallis and Dunn's tests; with the same process described in the previous paragraph. Not all repeatedly sampled colonies were successfully barcoded, hence the use of non-repeated measures tests, rather than the RM-MANOVAs used for phenotypic data. All data curation and statistical analyses were completed with R v4.1.2 in Rstudio v1.3.1073. Figures were generated and modified with a combination of ggplot2 v3.3.5 (Wickham, 2016) and InkScape v1.1 (https://inkscape.org).

3 Results

3.1 Environment

Guam's windward (East) and leeward (West) sides are characterized by a large disparity in average wave energy. Wave energy on Guam was highest from December to March with waves, on average, coming from the East year-round (Figure 1G). In 2021, Guam did not enter a formal coral bleaching warning (Liu et al., 2018; Skirving et al., 2020) nor was bleaching observed or reported locally. Water temperatures increased steadily from March to June, remaining stable during the following four months, although temperature change was relatively mild. Precipitation followed a similar trend (Figure 1H). May represented a seasonal transition with warming waters and decreasing wave energy; August was characterized by high water temperatures and low wave energy (Figures 1G, H).

3.2 Symbiodiniaceae cell density

Symbiodiniaceae cell density was relatively consistent and averaged 1.345×10^6 cells/cm^2 (SD: 5.455×10^6). Cell density only varied with time (RM-ANOVA: $t = 20.81$, $p = 0.042$). Notably, this was primarily driven by increased densities in South colonies during August (Figure 2A). All other factors demonstrated relatively low predictability for data structure (RM-ANOVA: Site: $t = 0.917$, $p = 0.44$; Time : Site: $t = 2.99$, $p = 0.159$; Site : Plot: $t = 0.758, 0.516$; Time : Site:Plot: $t = 0.711; 0.528$) (Table S1). Dunn's tests did not reveal any obvious factorial structuring (Figure S1A). Cell density was not correlated to any phenotypic metric (Spearmans: RED: $\rho = 0.096$, $p = 0.299$; FSC: $\rho = 0.021$, $p = 0.822$; SSC: $\rho = 0.03$, $p = 0.742$).

3.3 Symbiodiniaceae phenotypic variation

Symbiodiniaceae phenotypic metrics were heavily influenced by time (RM-MANOVA: $t = 2165.490$, $p < 0.001$), site (RM-MANOVA: $t = 4859.680$, $p < 0.001$), and site within time (RM-MANOVA: $t = 18.661$, $p < 0.001$) (Table S2). Time was especially influential for cell phenotype across four sites (North, Northwest, West, and South) with low phenotypic variance in May and a wide phenotypic variance in August (Figures 2B–E), while the East site displayed a wide phenotypic variance at both sampling time points (Figure 2F). All phenotypic variables were correlated to each other (Spearman: RED-FSC: $\rho = 0.38$, $p < 0.001$; RED-SSC: $\rho = 0.37$, $p < 0.001$; FSC-SSC: $\rho = 0.54$, $p < 0.001$).

Red fluorescence (photopigment abundance) was most influenced by site (RM-ANOVA: $t = 291.668$, $p < 0.001$); although it was also influenced by time (RM-ANOVA: $t = 1056.040$; $p = 0.002$) (Table S2). Generally, red fluorescence declined from May to August, aside from a few plot-specific scenarios, while sites showed a more complex, case-specific partitioning of statistical groups (Figure S1B). Side scatter (cell roughness) displayed similar trends of case-specific partitioning but was especially influenced by site within time (RM-ANOVA: $t = 86.503$, $p < 0.001$) and did not show any obvious large-scale pattern (Figure S1C). Forward scatter (cell size), by contrast, showed strong structuring with Site within Time (RM-ANOVA: $t = 322.342$, $p < 0.001$), and displayed comparatively little within site data variation (Table S2; Figure S1).

3.4 Symbiodiniaceae assemblage community composition

Symbiodiniaceae communities of *A. pulchra* were largely dominated by *Cladocopium* C40 (Figure 3A). ITS2 type

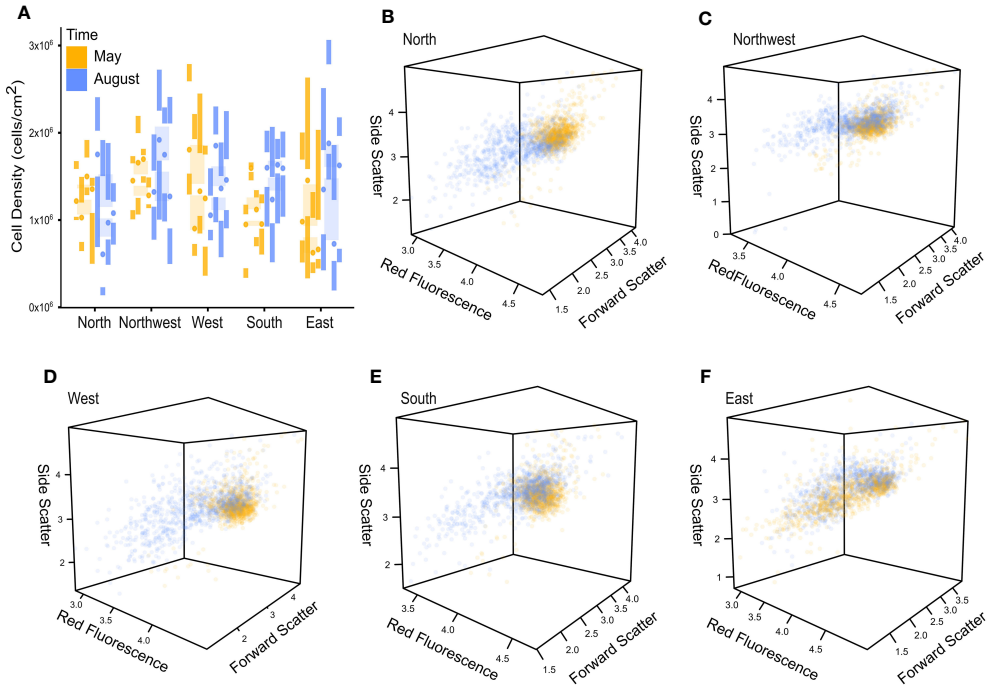

FIGURE 2
Cell density and phenotypic variance plots colored for repeated temporal sampling (May & August). **(A)** Cell density illustrated no pattern, as visualized by Tufte's box plots summarized to the plot level within each site and colored across temporal sampling points. **(B–F)** Phenotypic variance illustrates a temporal pattern, as visualized by three-dimensional dot plots for North **(B)**, Northwest **(C)**, West **(D)**, South **(E)**, and East **(F)** Symbiodiniaceae assemblages.

biodiversity and beta-diversity dispersion was determined by site (PERMANOVA: $F = 88.793$, $p = 0.001$; PERMDISP: $F = 11.725$, $p < 0.001$) and not by time (PERMANOVA: $F = 0.437$, $p = 0.761$; PERMDISP: $F = 0.014$, $p = 0.906$) (Figure 3; Table S3). ITS2 type profiles showed Symbiodiniaceae community overlap along Guam's western coast, while southern and eastern ITS2 type profiles were distinct (Figure 3).

Pairwise permutation tests revealed North as an outlier, the only site with a *Durusdinium* ITS2 type profile. A pairwise permutation test of the North site across time points indicated that communities were not statistically differentiated between sampling time points (PERM: $F = 0.543$, $p = 0.494$); however, plot-specific data suggested a *Cladocopium* to *Durusdinium* partitioning from nearshore to farshore colonies, with *Durusdinium* being more common nearshore (Figure 4).

3.5 Genotype-phenotype association

As discussed in previous sections, only the North site showed co-dominance of *Cladocopium* and *Durusdinium* ITS2 type profiles (Figure 3). Therefore, each colony with a successfully identified ITS2 type profile was compared to evaluate whether ITS2-type profiles were associated with phenotypic variance (Figure 4). Independent from plot, type profiles did not differ in cell density (Kruskal-Wallis: $X^2 = 5.760$, $df = 2$, $p = 0.056$) (Figure 4A). Plot-specific measurements illustrated a general increase in cell density from nearshore to farshore corals (Figure 4B), although accompanied by high variance. Although neighboring colonies with different ITS2 types (*Durusdinium* vs. *Cladocopium*) displayed different phenotypic profiles (e.g. colonies in Plots 2 and 3) (Figures 4C–E), neighboring colonies of the same ITS2 types (*Cladocopium* vs. *Cladocopium* or *Durusdinium* vs. *Durusdinium*) also demonstrated phenotypic differences (e.g. colonies in Plots 1, 3, and 4) (Figures 4C–E), indicating an alternative influence on phenotypic variance.

4 Discussion

We set out to identify whether seasonal phenotypic change and site-related phenotypic variation of Symbiodiniaceae assemblages is a product of symbiont shuffling or cellular plasticity. Therefore, we used flow cytometric phenotypic profiling to characterize the phenotypes of thousands of cells within each *Acropora pulchra* colony alongside ITS2 metabarcoding to identify Symbiodiniaceae clade and community composition. Combining phenotypic profiling with ITS2 metabarcoding provided the resolution to partition cellular plasticity and symbiont shuffling. Although environmental change between timepoints was relatively mild, flow cytometry revealed clear spatiotemporally structured phenotypic variation (Figures 2B–F). In conjunction with the geographic structuring of ITS2 biodiversity (Figure 3) and stable cell densities (Figure 2A), our data suggests that cellular plasticity of Symbiodiniaceae was responsible for changes in phenotypic variation.

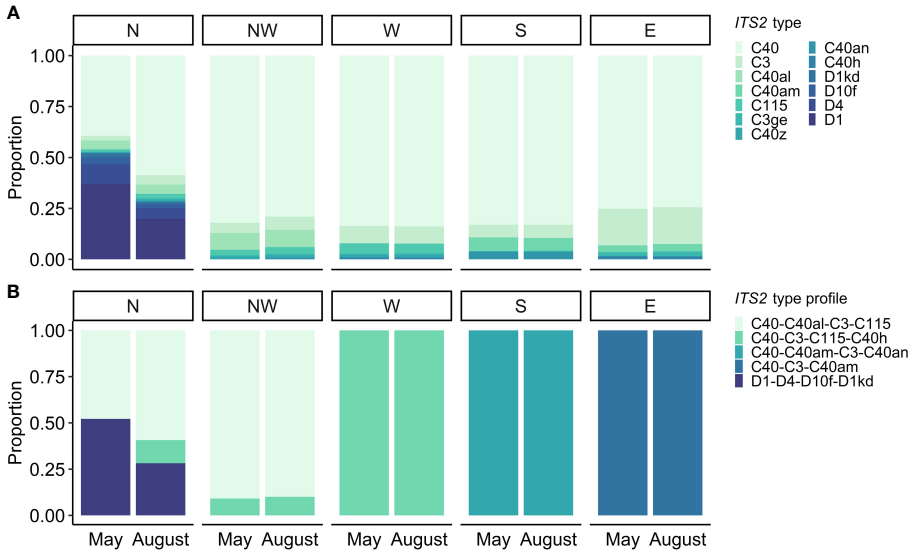

FIGURE 3
ITS2 type diversity **(A)** and ITS2 type profiles **(B)** from spatiotemporal sampling across five sites (North, Northwest, West, South, and East) and two timepoints (May and August).

4.1 Symbiodiniaceae community patterns

In *Acropora*, Symbiodiniaceae are acquired from the environment (Baird et al., 2009), and *Acropora* species are often thought to harbor more flexible and diverse symbiont assemblages than other coral genera (Rouzé et al., 2017; Qin et al., 2019). However, we found that *A. pulchra*-associated Symbiodiniaceae ITS2 types were geographically structured and temporally stable (Figure 3). Although the high fidelity *A. pulchra*-associated Symbiodiniaceae may be surprising, this result is consistent with previous studies from Guam. For example, Rios (2020) found Guam's *A. pulchra*-associated Symbiodiniaceae assemblages dominated by *Cladocopium*, with only *A. pulchra* from Saipan and northern Guam containing *Durusdinium*-dominated colonies. Additionally, the long-term monitoring of Symbiodiniaceae communities found high stability and colony-level specificity of *A. pulchra*-associated Symbiodiniaceae in French Polynesia (Rouzé et al., 2019).

The dominance of thermotolerant Symbiodiniaceae, *Cladocopium* C40 and *Durusdinium* D1, in *A. pulchra* on Guam's reef flats indicate the selection of resilient corals following mass coral bleaching and mortality. Both *Cladocopium* C40 and *Durusdinium* D1 represent important lineages associated with reduced coral bleaching rates and increased coral survival following stress (Jones et al., 2008; Mieog et al., 2009; Rouzé et al., 2017; Qin et al., 2019). Guam experienced four major coral bleaching events over the last decade leading to an estimated 60% reduction of coral cover between 2013 and 2017 (Raymundo et al., 2019). At many sites around Guam, *A. pulchra* populations experienced 50-100% mortality, yet, among acroporids, *A. pulchra* remains the dominant reef-building coral on Guam's reef flats (Raymundo et al., 2017; Raymundo et al., 2019). The nearshore to farshore partitioning of *Durusdinium* D1 to *Cladocopium* C40 dominated *A. pulchra* colonies may be the result of microhabitat adaptation to long term chronic stressors or environmental conditions (e.g. differences in water flow observed across Guam's reef flats; Fifer et al., 2021), a hypothesis that ought to be tested with additional targeted sampling.

Under extreme environmental stress, successful acclimation may be caused by symbiont shuffling, the turnover of symbiont community composition (Buddemeier and Fautin, 1993; Baker, 2003; Jones et al., 2008; Zhu et al., 2022). *Durusdinium* D1 may have been selected for its higher tolerance to warmer nearshore waters (Stat et al., 2008; Keshavmurthy et al., 2014; Silverstein et al., 2017). Additionally, selection for Symbiodiniaceae genotypes may have led to microhabitat adaptation that cannot be detected using ITS2 metabarcoding. For example, signatures of selection were identified from transcriptomes of Symbiodiniaceae living in acidic waters of CO_2 seeps (Leiva et al., 2023). The combination of *A. pulchra* host clonality (Rios, 2020), geographical structuring of Symbiodiniaceae in Guam and the surrounding region (Davies et al., 2020; Rios, 2020; Current Study), and the temporal stability of Symbiodiniaceae community composition (Rouzé et al., 2019; Current Study) point to the importance of phenotypic plasticity as an acclimation mechanism for *A. pulchra* and its Symbiodiniaceae assemblage. *A. pulchra's* fidelity for putatively thermotolerant *Cladocopium* C40 and *Durusdinium* D1 may have allowed *A. pulchra* to persist through repeated severe coral bleaching, but the full acclimation potential of this coral remains to be explored.

4.2 Phenotypic variation and plasticity

Species of Symbiodiniaceae have been experimentally shown to display varying degrees of plasticity to respond to environmental change (Mansour et al., 2018); therefore, we expected that phenotypic

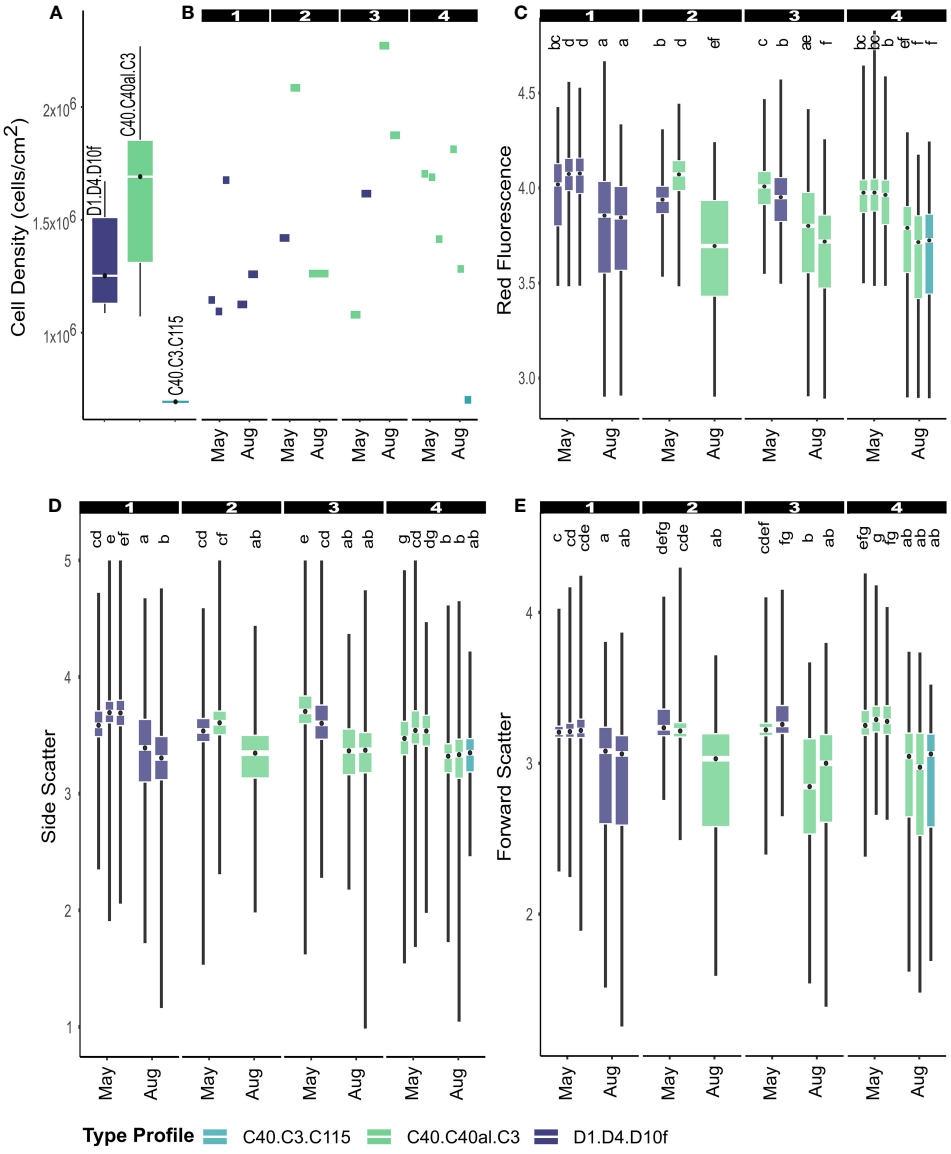

FIGURE 4
Cell density **(A, B)** and phenotypic measurements **(C–E)** were mapped to samples from the North site with known ITS2 type profiles. Sampled plots spanned across the reef flat from nearshore to farshore (1-4) (Figure 1B). Box plots **(C–E)** correspond to different colonies sampled within their respective plots (Figure 1). Letters above each boxplot **(C–E)** indicate statistical groupings (p<0.001).

variation of a coral-associated Symbiodiniaceae assemblage would differ between different Symbiodiniaceae assemblages. Between time points, flow cytometry revealed that most *Acropora pulchra* colonies had a low phenotypic variance of Symbiodiniaceae in May and high phenotypic variance in August (Figure 2). In conjunction, with temporally stable ITS2 community compositions, we have strong evidence for temporal cellular plasticity. However, phenotypic variance was also influenced by site (Table S3).

The overall taxonomic homogeneity of community compositions made determining the influence of Symbiodiniaceae identities on spatial phenotypic differences difficult. Only the North site provided any insight on the influence of Symbiodiniaceae community composition given the codominance of two ITS2 type profiles: (1) *Durisdinium* D1-dominated and (2) *Cladocopium* C40-dominated (Figure 3). After mapping ITS2-type profiles of each colony to their respective phenotypic profiles, colonies from nearshore (*Durusdinium* D1-dominated) to farshore (*Cladocopium* C40-dominated) displayed some mild differences in phenotypic characteristics, such as the higher abundance of photopigments (high red fluorescence) in nearshore colonies (Figure 4C). However, the phenotypic variance between neighboring *Durusdinium* and *Cladocopium*-dominated colonies (e.g. colonies in Plots 2 and 3) was no different than neighboring colonies of the same ITS2 types (e.g. colonies in Plots 1, 3, and 4) (Figure 4). Although flow cytometry-derived phenotypic metrics display high variation, high sampling size (>1000 cells) makes comparative results robust (Anthony et al., 2023). Therefore, the data indicate that phenotypic variation between colonies is most likely caused by the cellular plasticity of Symbiodiniaceae, and not by differences in community composition.

5 Conclusion

Symbiodiniaceae communities of Guam's *A. pulchra* populations did not display changes in cell densities or community composition shuffling (Figures 2A, 3). Instead, *A. pulchra*'s Symbiodiniaceae communities were geographically structured by sampling location (Figure 3), similar to the geographic structuring of acroporid Symbiodiniaceae communities reported previously. Flow cytometric phenotypic profiling revealed that time and site-specific phenotypic differences were likely caused by plasticity of Symbiodiniaceae cells (Figures 2, 4). The implementation and expansion of flow cytometric phenotypic profiling within the framework presented here, for example by characterizing Symbiodiniaceae phenotypic variation with higher temporal resolution and samples from extreme events, has the potential to provide important insights into the mechanisms, dynamics, and limits of Symbiodiniaceae acclimation *in situ*.

Data availability statement

The datasets presented in this study can be found in online repositories. The names of the repository/repositories and accession number(s) can be found below: www.symportal.org, 20220419_GuamWild_bentlage. NCBI Genbank Bioproject, PRJNA104307; github.com, AnthonyCuog/SpatiotemporalProfiling.

Ethics statement

Collection permits were issued by Guam's Division of Aquatic & Wildlife Resources. The study was conducted in accordance with the local legislation and institutional requirements.

Author contributions

CJA: Conceptualization, Data curation, Formal Analysis, Investigation, Methodology, Software, Validation, Visualization, Writing – review & editing, Writing – original draft. CL: Data curation, Formal Analysis, Investigation, Methodology, Validation, Writing – review & editing. BMT: Formal Analysis, Supervision, Writing – review & editing. BB: Funding acquisition, Investigation, Methodology, Project administration, Resources, Supervision, Validation, Writing – review & editing.

Funding

The author(s) declare financial support was received for the research, authorship, and/or publication of this article. This work was directly supported by Guam NSF EPSCoR through the National Science Foundation (award OIA-1946352). Wave data was provided by the Pacific Islands Ocean Observing System (PacIOOS) (www.pacioos.org), which is a part of the U.S. Integrated Ocean Observing System (IOOS), funded in part by National Oceanic and Atmospheric Administration (NOAA) (awards #NA16NOS0120024 and #NA21NOS0120091).

Acknowledgments

We wish to thank Dr. Cheryl Ames, Dr. Héloïse Rouzé, and Dr. Shinichiro Maruyama for providing their expertise and mentorship. We would also like to thank Marine Laboratory boat captain, Jonathan "Nanny" Perez, for assisting with field collections in Cocos Lagoon, and the Ritidian Eco Beach Resort for providing land access to the pristine reef flats of Urunao.

Conflict of interest

The authors declare that the research was conducted in the absence of any commercial or financial relationships that could be construed as a potential conflict of interest.

Publisher's note

Supplementary material

The Supplementary Material for this article can be found online at: https://www.frontiersin.org/articles/10.3389/fevo.2023.1288596/full#supplementary-material

References

Anthony, C. J., Lock, C. C., and Bentlage, B. (2023). Rapid, high-throughput phenotypic profiling of endosymbiotic dinoflagellates (Symbiodiniaceae) using benchtop flow cytometry. *PloS One* 18, e0290649. doi: 10.1371/journal.pone.0290649

Apprill, A. M., Bidigare, R. R., and Gates, R. D. (2007). Visibly healthy corals exhibit variable pigment concentrations and symbiont phenotypes. *Coral Reefs* 26, 387–397. doi: 10.1007/s00338-007-0209-y

Baird, A. H., Guest, J. R., and Willis, B. L. (2009). Systematic and biogeographical patterns in the reproductive biology of scleractinian corals. *Annu. Rev. Ecol. Evol. Syst.* 40, 551–571. doi: 10.1146/annurev.ecolsys.110308.120220

Baker, A. C. (2003). Flexibility and specificity in coral-algal symbiosis: diversity, ecology, and biogeography of *Symbiodinium*. *Annu. Rev. Ecol. Evol. Syst.* 34, 661–689. doi: 10.1146/annurev.ecolsys.34.011802.132417

Baker, A. C., Starger, C. J., McClanahan, T. R., and Glynn, P. W. (2004). Coral reefs: corals' adaptive response to climate change. *Nature* 430, 741. doi: 10.1038/430741a

Baker, D. M., Freeman, C. J., Wong, J. C. Y., Fogel, M. L., and Knowlton, N. (2018). Climate change promotes parasitism in a coral symbiosis. *ISME J.* 12, 921–930. doi: 10.1038/s41396-018-0046-8

Berkelmans, R., and van Oppen, M. J. H. (2006). The role of zooxanthellae in the thermal tolerance of corals: a "nugget of hope" for coral reefs in an era of climate change. *Proc. Biol. Sci.* 273, 2305–2312. doi: 10.1098/rspb.2006.3567

Brook, G. (1891). Descriptions of new species of *Madrepora* in the collections of the British Museum. *Ann. Mag. Nat. Hist.* 8, 458–471. doi: 10.1080/00222939109459223

Brown, B. E. (1997). Coral bleaching: causes and consequences. *Coral Reefs* 16, S129–S138. doi: 10.1007/s003380050249

Buddemeier, R. W., and Fautin, D. G. (1993). Coral Bleaching as an Adaptive Mechanism: A testable hypothesis. *Bioscience* 43, 320–326. doi: 10.2307/1312064

Camp, E. F., Edmondson, J., Doheny, A., Rumney, J., Grima, A. J., Huete, A., et al. (2019). Mangrove lagoons of the Great Barrier Reef support coral populations persisting under extreme environmental conditions. *Mar. Ecol. Prog. Ser.* 625, 1–14. doi: 10.3354/meps13073

Cignoni, P., Callieri, M., and Corsini, M. (n. d.). Meshlab: an open-source mesh processing tool. *Eurographics Italian.*. doi: 10.2312/localchapterevents.italchap.italianchapconf2008.129-136/129-136

Cooper, E. D., Bentlage, B., Gibbons, T. R., Bachvaroff, T. R., and Delwiche, C. F. (2014). Metatranscriptome profiling of a harmful algal bloom. *Harmful Algae* 37, 75–83. doi: 10.1016/j.hal.2014.04.016

Cooper, T. F., Ulstrup, K. E., Dandan, S. S., Heyward, A. J., Kühl, M., Muirhead, A., et al. (2011). Niche specialization of reef-building corals in the mesophotic zone: metabolic trade-offs between divergent *Symbiodinium* types. *Proc. Biol. Sci.* 278, 1840–1850. doi: 10.1098/rspb.2010.2321

Davies, S. W., Moreland, K. N., Wham, D. C., Kanke, M. R., and Matz, M. V. (2020). *Cladocopium* community divergence in two *Acropora* coral hosts across multiple spatial scales. *Molec. Ecol.* 00, 1–14. doi: 10.1111/mec.15668

Eckert, R. J., Reaume, A. M., Sturm, A. B., Studivan, M. S., and Voss, J. D. (2020). Depth influences symbiodiniaceae associations among *Montastraea cavernosa* corals on the Belize barrier reef. *Front. Microbiol.* 11, 518. doi: 10.3389/fmicb.2020.00518

Ezzat, L., Fine, M., Maguer, J.-F., Grover, R., and Ferrier-Pagès, C. (2017). Carbon and nitrogen acquisition in shallow and deep holobionts of the scleractinian coral *S. pistillata*. *Front. Mar. Sci.* 4. doi: 10.3389/fmars.2017.00102

Fabricius, K. E., Mieog, J. C., Colin, P. L., Idip, D., and van Oppen, M. J. H. (2004). Identity and diversity of coral endosymbionts (zooxanthellae) from three Palauan reefs with contrasting bleaching, temperature and shading histories. *Mol. Ecol.* 13, 2445–2458. doi: 10.1111/j.1365-294X.2004.02230.x

Falkowski, P. G., Dubinsky, Z., Muscatine, L., and Porter, J. W. (1984). Light and the bioenergetics of a symbiotic coral. *Bioscience* 34, 705–709. doi: 10.2307/1309663

Fifer, J., Bentlage, B., Lemer, S., Fujimura, A. G., Sweet, M., and Raymundo, L. J. (2021). Going with the flow: How corals in high-flow environments can beat the heat. *Molec. Ecol.* 30, 2009–2024. doi: 10.1111/mec.15869

Fine, M., Gildor, H., and Genin, A. (2013). A coral reef refuge in the Red Sea. *Glob. Change Biol.* 19, 3640–3647. doi: 10.1111/gcb.12356

Frade, P. R., De Jongh, F., Vermeulen, F., van Bleijswijk, J., and Bak, R. P. M. (2008). Variation in symbiont distribution between closely related coral species over large depth ranges. *Mol. Ecol.* 17, 691–703. doi: 10.1111/j.1365-294X.2007.03612.x

Friedrich, S., Konietschke, F., and Pauly, M. (2019). Resampling-based analysis of multivariate data and repeated measures designs with the R package MANOVA.RM. *R J.* 11, 380.

Friedrich, S., Konietshke, F., and Pauly, M. (2022). *MANOVA.RM: Resampling-Based Analysis of Multivariate Data and Repeated Measures Designs*. doi: 10.32614/RJ-2019-051

Gault, J. A., Bentlage, B., Huang, D., and Kerr, A. M. (2021). Lineage-specific variation in the evolutionary stability of coral photosymbiosis. *Sci. Adv.* 7, eabh4243. doi: 10.1126/sciadv.abh4243

Goulet, T. L. (2006). Most corals may not change their symbionts. *Mar. Ecol. Prog. Ser.* 321, 1–7. doi: 10.3354/meps321001

Hennige, S. J., Smith, D. J., Perkins, R., Consalvey, M., Paterson, D. M., and Suggett, D. J. (2008). Photoacclimation, growth and distribution of massive coral species in clear and turbid waters. *Mar. Ecol. Prog. Ser.* 369, 77–88. doi: 10.3354/meps07612

Hoadley, K. D., Lockridge, G., McQuagge, A., Pahl, K. B., Lowry, S., Wong, S., et al. (2023). A phenomic modeling approach for using chlorophyll-a fluorescence-based measurements on coral photosymbionts. *Front. Mar. Sci.* 10. doi: 10.3389/fmars.2023.1092202

Howe-Kerr, L. I., Bachelot, B., Wright, R. M., Kenkel, C. D., Bay, L. K., and Correa, A. M. S. (2020). Symbiont community diversity is more variable in corals that respond poorly to stress. *Glob. Change Biol.* 26, 2220–2234. doi: 10.1111/gcb.14999

Hughes, T. P., Barnes, M. L., Bellwood, D. R., Cinner, J. E., Cumming, G. S., Jackson, J. B. C., et al. (2017). Coral reefs in the anthropocene. *Nature* 546, 82–90. doi: 10.1038/nature22901

Hume, B. C. C., Smith, E. G., Ziegler, M., Warrington, H. J. M., Burt, J. A., LaJeunesse, T. C., et al. (2019). SymPortal: A novel analytical framework and platform for coral algal symbiont next-generation sequencing ITS2 profiling. *Mol. Ecol. Resour.* 19, 1063–1080. doi: 10.1111/1755-0998.13004

Hume, B. C. C., Ziegler, M., Poulain, J., Pochon, X., Romac, S., Boissin, E., et al. (2018). An improved primer set and amplification protocol with increased specificity and sensitivity targeting the *Symbiodinium* ITS2 region. *PeerJ* 6, e4816. doi: 10.7717/peerj.4816

Iglesias-Prieto, R., Beltrán, V. H., LaJeunesse, T. C., Reyes-Bonilla, H., and Thomé, P. E. (2004). Different algal symbionts explain the vertical distribution of dominant reef corals in the eastern Pacific. *Proc. Biol. Sci.* 271, 1757–1763. doi: 10.1098/rspb.2004.2757

Johnsen, G., Samset, O., Granskog, L., and Sakshaug, E. (1994). *In vivo* absorption characteristics in 10 classes of bloom-forming phytoplankton: taxonomic characteristics and responses to photoadaptation by means of discriminant and HPLC analysis. *Mar. Ecol. Prog. Ser.* 105, 149–157. doi: 10.3354/meps105149

Jones, A. M., Berkelmans, R., van Oppen, M. J. H., Mieog, J. C., and Sinclair, W. (2008). A community change in the algal endosymbionts of a scleractinian coral following a natural bleaching event: field evidence of acclimatization. *Proc. Biol. Sci.* 275, 1359–1365. doi: 10.1098/rspb.2008.0069

Jones, R. J., and Yellowlees, D. (1997). Regulation and control of intracellular algae (= zooxanthellae) in hard corals. *Philos. Trans. R. Soc Lond. B Biol. Sci.* 352, 457–468. doi: 10.1098/rstb.1997.0033

Kassambara, A. (2022). *Rstatix: Pipe-friendly framework for basic statistical tests. R package version 0.7.1.*

Keshavmurthy, S., Meng, P.-J., Wang, J.-T., Kuo, C.-Y., Yang, S.-Y., Hsu, C.-M., et al. (2014). Can resistant coral-*Symbiodinium* associations enable coral communities to survive climate change? A study of a site exposed to long-term hot water input. *PeerJ* 2, e327. doi: 10.7717/peerj.327

Krediet, C. J., DeNofrio, J. C., Caruso, C., Burriesci, M. S., Cella, K., and Pringle, J. R. (2015). Rapid, precise, and accurate counts of *Symbiodinium* cells using the guava flow cytometer, and a comparison to other methods. *PloS One* 10, e0135725. doi: 10.1371/journal.pone.0135725

LaJeunesse, T. C., Parkinson, J. E., Gabrielson, P. W., Jeong, H. J., Reimer, J. D., Voolstra, C. R., et al. (2018). Systematic revision of symbiodiniaceae highlights the antiquity and diversity of coral endosymbionts. *Curr. Biol.* 28, 2570–2580.e6. doi: 10.1016/j.cub.2018.07.008

LaJeunesse, T. C., Pettay, D. T., Sampayo, E. M., Phongsuwan, N., Brown, B., Obura, D. O., et al. (2010). Long-standing environmental conditions, geographic isolation and host-symbiont specificity influence the relative ecological dominance and genetic diversification of coral endosymbionts in the genus *Symbiodinium*. *J. Biogeogr.* 37, 785–800. doi: 10.1111/j.1365-2699.2010.02273.x

Lee, C. S., Yeo, Y. S. W., and Sin, T. M. (2012). Bleaching response of *Symbiodinium* (zooxanthellae): determination by flow cytometry. *Cytometry A* 81, 888–895. doi: 10.1002/cyto.a.22111

Leiva, C., Pérez-Portela, R., and Lemer, C. (2023). Genomic signatures suggesting adaptation to ocean acidification in a coral holobiont from volcanic CO_2 seeps. *Commun. Biol.* 6, 769. doi: 10.1038/s42003-023-05103-7

Lesser, M. P. (1996). Elevated temperatures and ultraviolet radiation cause oxidative stress and inhibit photosynthesis in symbiotic dinoflagellates. *Limnol. Oceanogr.* 41, 271–283. doi: 10.4319/lo.1996.41.2.0271

Lesser, M. P., Slattery, M., Stat, M., Ojimi, M., Gates, R. D., and Grottoli, A. (2010). Photoacclimatization by the coral *Montastraea cavernosa* in the mesophotic zone: light, food, and genetics. *Ecology* 91, 990–1003. doi: 10.1890/09-0313.1

Liu, G., Eakin, C. M., Chen, M., Kumar, A., de la Cour, J. L., Heron, S. F., et al. (2018). Predicting heat stress to inform reef management: NOAA coral reef watch's 4-month coral bleaching outlook. *Front. Mar. Sci.* 5. doi: 10.3389/fmars.2018.00057

Mangiafico, S. (2023) *rcompanion: Functions to Support Extension Education Program Evaluation*. Available at: https://CRAN.R-project.org/package=rcompanion.

Mansour, J. S., Pollock, F. J., Díaz-Almeyda, E., Iglesias-Prieto, R., and Medina, M. (2018). Intra- and interspecific variation and phenotypic plasticity in thylakoid membrane properties across two *Symbiodinium* clades. *Coral Reefs* 37, 841–850. doi: 10.1007/s00338-018-1710-1

Mantoura, R. F. C., and Llewellyn, C. A. (1983). The rapid determination of algal chlorophyll and carotenoid pigments and their breakdown products in natural waters by reverse-phase high-performance liquid chromatography. *Anal. Chim. Acta* 151, 297–314. doi: 10.1016/S0003-2670(00)80092-6

Martinez Arbizu, P. (2017). *pairwiseAdonis: Pairwise Multilevel Comparison using Adonis.*

Matthews, J. L., Crowder, C. M., Oakley, C. A., Lutz, A., Roessner, U., Meyer, E., et al. (2017). Optimal nutrient exchange and immune responses operate in partner specificity in the cnidarian-dinoflagellate symbiosis. *Proc. Natl. Acad. Sci. U. S. A.* 114, 13194–13199. doi: 10.1073/pnas.1710733114

Menne, M. J., Durre, I., Vose, R. S., Gleason, B. E., and Houston, T. G. (2012). An overview of the global historical climatology network-daily database. *J. Atmos. Ocean. Technol.* 29, 897–910. doi: 10.1175/JTECH-D-11-00103.1

Mieog, J. C., Olsen, J. L., Berkelmans, R., Bleuler-Martinez, S. A., Willis, B. L., and van Oppen, M. J. H. (2009). The roles and interactions of symbiont, host and environment in defining coral fitness. *PloS One* 4, e6364. doi: 10.1371/annotation/e06b31ef-6b29-44ae-aec1-1740daa93f4b

Mullaney, P. F., Van Dilla, M. A., Coulter, J. R., and Dean, P. N. (1969). Cell sizing: a light scattering photometer for rapid volume determination. *Rev. Sci. Instrum.* 40, 1029–1032. doi: 10.1063/1.1684143

Muscatine, L., Falkowski, P. G., Porter, J. W., and Dubinsky, Z. (1984). Fate of photosynthetic fixed carbon in light- and shade-adapted colonies of the symbiotic coral. *Stylophora pistillata*. *Proc. R. Soc Lond.* 222, 181–202. doi: 10.1098/rspb.1984.0058

Nitschke, M. R., Gardner, S. G., Goyen, S., Fujise, L., Camp, E. F., Ralph, P. J., et al. (2018). Utility of photochemical traits as diagnostics of thermal tolerance amongst great barrier reef corals. *Front. Mar. Sci.* 5. doi: 10.3389/fmars.2018.00045

Oakley, C. A., Schmidt, G. W., and Hopkinson, B. M. (2014). Thermal responses of *Symbiodinium* photosynthetic carbon assimilation. *Coral Reefs* 33, 501–512. doi: 10.1007/s00338-014-1130-9

Ogle, D. H., Doll, J. C., Wheeler, P., and Dinno, A. (2022). *FSA: Fisheries Stock Analysis. R package version 0.9.3.*

Oksanen, J., Blanchet, F. G., Friendly, M., Kindt, R., Legendre, P., Minchin, P. R., et al. (2019). *Vegan: Community Ecology Package.*

Oliveira, C. Y. B., Abreu, J. L., Santos, E. P., Matos, Â.P., Tribuzi, G., Oliveira, C. D. L., et al. (2022). Light induces peridinin and docosahexaenoic acid accumulation in the dinoflagellate *Durusdinium glynnii*. *Appl. Microbiol. Biotechnol.* 106, 6263–6276. doi: 10.1007/s00253-022-12131-6

Parkinson, J. E., Coffroth, M. A., and LaJeunesse, T. C. (2015). New species of Clade B Symbiodinium (Dinophyceae) from the greater Caribbean belong to different functional guilds: *S. aenigmaticum* sp. nov., *S. antillogorgium* sp. nov., *S. endomadracis* sp. nov., and *S. pseudominutum* sp. nov. *J. Phycol.* 51, 850–858. doi: 10.1111/jpy.12340

Qin, Z., Yu, K., Chen, B., Wang, Y., Liang, J., Luo, W., et al. (2019). Diversity of Symbiodiniaceae in 15 coral species from the Southern South China Sea: Potential relationship with coral thermal adaptability. *Front. Microbiol.* 10, 2343. doi: 10.3389/fmicb.2019.02343

Raymundo, L. J., Burdick, D., Hoot, W. C., Miller, R. M., Brown, V., Reynolds, T., et al. (2019). Successive bleaching events cause mass coral mortality in Guam, Micronesia. *Coral Reefs* 38, 677–700. doi: 10.1007/s00338-019-01836-2

Raymundo, L. J., Burdick, D., Lapacek, V. A., Miller, R., and Brown, V. (2017). Anomalous temperatures and extreme tides: Guam staghorn *Acropora* succumb to a double threat. *Mar. Ecol. Prog. Ser.* 564, 47–55. doi: 10.3354/meps12005

Rios, D. (2020). *The population genetic structure of Acropora pulchra in Guam*. Master's Thesis (Mangilao, Guam: University of Guam).

Roche, R. C., Williams, G. J., and Turner, J. R. (2018). Towards developing mechanistic understanding of coral reef resilience to thermal stress across multiple scales. *Curr. Clim. Change Rep.* 4, 51–64. doi: 10.1007/s40641-018-0087-0

Rouzé, H., Lecellier, G., Pochon, X., Torda, G., and Berteaux-Lecellier, V. (2019). Unique quantitative Symbiodiniaceae signature of coral colonies revealed through spatio-temporal survey in Moorea. *Sci. Rep.* 9, 7921. doi: 10.1038/s41598-019-44017-5

Rouzé, H., Lecellier, G. J., Saulnier, D., Planes, S., Gueguen, Y., Wirshing, H. H., et al. (2017). An updated assessment of Symbiodinium spp. that associate with common scleractinian corals from Moorea (French Polynesia) reveals high diversity among background symbionts and a novel finding of clade B. *PeerJ* 5, e2856. doi: 10.7717/peerj.2856

Sawall, Y., Al-Sofyani, A., Banguera-Hinestroza, E., and Voolstra, C. R. (2014). Spatio-temporal analyses of Symbiodinium physiology of the coral *Pocillopora verrucosa* along large-scale nutrient and temperature gradients in the Red Sea. *PloS One* 9, e103179. doi: 10.1371/journal.pone.0103179

Shapiro, H. M. (2003). *Practical Flow Cytometry* 4th edition (United States of America: John Wiley & Sons).

Silverstein, R. N., Cunning, R., and Baker, A. C. (2017). Tenacious D: *Symbiodinium* in clade D remain in reef corals at both high and low temperature extremes despite impairment. *J. Exp. Biol.* 220, 1192–1196. doi: 10.1242/jeb.148239

Skirving, W., Marsh, B., de la Cour, J., Liu, G., Harris, A., Maturi, E., et al. (2020). CoralTemp and the coral reef watch coral bleaching heat stress product suite version 3.1. *Remote Sens.* 12, 3856. doi: 10.3390/rs12233856

Stat, M., Morris, E., and Gates, R. D. (2008). Functional diversity in coral-dinoflagellate symbiosis. *Proc. Natl. Acad. Sci. U. S. A.* 105, 9256–9261. doi: 10.1073/pnas.0801328105

Steen, H. B. (1980). Further developments of a microscope-based flow cytometer: light scatter detection and excitation intensity compensation. *Cytometry* 1, 26–31. doi: 10.1002/cyto.990010107

Suggett, D. J., Kikuchi, R. K. P., Oliveira, M. D. M., Spanó, S., Carvalho, R., and Smith, D. J. (2012). Photobiology of corals from Brazil's near-shore marginal reefs of Abrolhos. *Mar. Biol.* 159, 1461–1473. doi: 10.1007/s00227-012-1925-6

Swain, T. D., Lax, S., Backman, V., and Marcelino, L. A. (2020). Uncovering the role of Symbiodiniaceae assemblage composition and abundance in coral bleaching response by minimizing sampling and evolutionary biases. *BMC Microbiol.* 20, 124. doi: 10.1186/s12866-020-01765-z

Thornhill, D. J., Lewis, A. M., Wham, D. C., and LaJeunesse, T. C. (2014). Host-specialist lineages dominate the adaptive radiation of reef coral endosymbionts. *Evolution* 68, 352–367. doi: 10.1111/evo.12270

Tzur, A., Moore, J. K., Jorgensen, P., and Shapiro, H. M. (2011). Optimizing optical flow cytometry for cell volume-based sorting and analysis. *PloS One* 6, e16053. doi: 10.1371/journal.pone.0016053

Ulstrup, K. E., Hill, R., van Oppen, M. J. H., Larkum, A. W. D., and Ralph, P. J. (2008). Seasonal variation in the photo-physiology of homogeneous and heterogeneous *Symbiodinium* consortia in two scleractinian corals. *Mar. Ecol. Prog. Ser.* 361, 139–150. doi: 10.3354/meps07360

Voolstra, C. R., Buitrago-López, C., Perna, G., Cárdenas, A., Hume, B. C. C., Rädecker, N., et al. (2020). Standardized short-term acute heat stress assays resolve historical differences in coral thermotolerance across microhabitat reef sites. *Glob. Change Biol.* 26, 4328–4343. doi: 10.1111/gcb.15148

Warner, M., Chilcoat, G., McFarland, F., and Fitt, W. (2002). Seasonal fluctuations in the photosynthetic capacity of photosystem II in symbiotic dinoflagellates in the Caribbean reef-building coral *Montastraea*. *Mar. Biol.* 141, 31–38. doi: 10.1007/s00227-002-0807-8

Warner, M. E., Fitt, W. K., and Schmidt, G. W. (1996). The effects of elevated temperature on the photosynthetic efficiency of zooxanthellae *in-hospite* from four different species of reef coral: a novel approach. *Plant Cell Environ.* 19, 291–299. doi: 10.1111/j.1365-3040.1996.tb00251.x

Wickham, H. (2016). *ggplot2: Elegant Graphics for Data Analysis* (Springer). doi: 10.1007/978-3-319-24277-4_10

Xiang, T., Nelson, W., Rodriguez, J., Tolleter, D., and Grossman, A. R. (2015). *Symbiodinium* transcriptome and global responses of cells to immediate changes in light intensity when grown under autotrophic or mixotrophic conditions. *Plant J.* 82, 67–80. doi: 10.1111/tpj.12789

Zhu, W., Liu, X., Zhu, M., Li, X., Yin, H., Huang, J., et al. (2022). Responses of symbiodiniaceae shuffling and microbial community assembly in thermally stressed *Acropora hyacinthus*. *Front. Microbiol.* 13, 832081. doi: 10.3389/fmicb.2022.832081